RAA 2017 Vol. **17** No. **2**, 12 (10pp) doi: 10.1088/1674–4527/17/2/12

http://www.raa-journal.org *http://iopscience.iop.org/raa*

***R**esearch in*
***A**stronomy and*
***A**strophysics*

What is the right way to quench star formation in semi-analytic models of galaxy formation?

Yu Luo[1,2] and Xi Kang[1]

[1] Purple Mountain Observatory, the Partner Group of MPI für Astronomie, Nanjing 210008, China; *luoyu@pmo.ac.cn, kangxi@pmo.ac.cn*

[2] Graduate School, University of the Chinese Academy of Sciences, Beijing 100049, China

Received 2016 September 2; accepted 2016 October 16

Abstract Semi-analytic models of galaxy formation are powerful tools to study the evolution of a galaxy population in a cosmological context. However, most models overpredict the number of low-mass galaxies at high redshifts and the colors of model galaxies are not right in the sense that low-mass satellite galaxies are too red and centrals are too blue. The recent version of the L-Galaxies model by Henriques et al. (H15) is a step forward to solve these problems by reproducing the evolution of stellar mass function and the overall fraction of red galaxies. In this paper we compare the two model predictions of L-Galaxies (the other is Guo et al., G13) to SDSS data in detail. We find that in the H15 model the red fraction of central galaxies now agrees with the data due to their implementation of strong AGN feedback, but the stellar mass of centrals in massive halos is now slightly lower than what is indicated by the data. For satellite galaxies, the red fraction of low-mass galaxies ($\log M_*/M_\odot < 10$) also agrees with the data, but the color of massive satellites ($10 < \log M_*/M_\odot < 11$) is slightly bluer. The correct color of centrals and the bluer color of massive satellites indicate that quenching in massive satellites is not strong enough. We also find that there are too many red spirals and less bulge-dominated galaxies in both H15 and G13 models. Our results suggest that additional mechanisms, such as more minor mergers or disk instability, are needed to slightly increase the stellar mass of the central galaxy in massive galaxies, mainly in the bulge component, and bulge dominated galaxies will be quenched not only by minor mergers, but also by some other mechanisms.

Key words: galaxies: evolution — galaxies: formation — galaxies: star formation

1 INTRODUCTION

The standard cold dark matter model is now very successful in explaining structure formation in the universe from the very early beginning up to the present (see the review by Frenk & White 2012). The nature of dark matter and dark energy is one of the main science goals of the next generation of sky surveys, such as EUCLID and LSST. On the other hand, the wealth of data on galaxies from ongoing and future surveys is very useful for the study of galaxy formation and evolution. Although many efforts have been made to model galaxy formation, it is fair to say that there is no model which can simultaneously reproduce the various properties of galaxies from local surveys well, for example the Sloan Digital Sky Survey (SDSS). In that sense, our understanding of galaxy formation lags behind our knowledge about the evolution of dark structure, which is accessible using large N-body simulations (e.g., Springel et al. 2005).

Hydrodynamical simulation and semi-analytic models (SAMs) are powerful physical tools to study galaxy formation and evolution in a cosmological context. State-of-the-art hydrodynamical simulations are now able to reproduce many properties of galaxies in typical cosmological volumes (e.g., Vogelsberger et al. 2014; Schaye et al. 2015), but due to the expensive cost of running huge and high-resolution hydrodynamical simulations, it is difficult to test how galaxy properties correspond to adopted physical models of star formation and feedback. Unlike hydrodynamical simulations, SAMs are based on N-body simulations, and they implement simple phenomenological descriptions of the physical processes in-

volved in galaxy formation, such as cosmic reionization, hot gas cooling and cold gas infall, star formation and metal production, supernova (SN) feedback, gas stripping and tidal disruption of satellites, galaxy mergers, bulge formation, black hole growth and active galactic nucleus (AGN) feedback. SAMs have developed quickly in the past few decades and most of the basic features of galaxy formation are already included in earlier versions of SAMs (e.g. White & Frenk 1991; Somerville & Primack 1999; Kang et al. 2005; Bower et al. 2006; Somerville et al. 2008). The main goal of SAMs is to reproduce the statistical properties of galaxies seen in the data as much as possible. A SAM is not only intended to make predictions of new observations, but more importantly to test our understanding of a physical model of galaxy formation in a fast and easy way.

SAMs have achieved great progress in recent years. They can reproduce the observed local stellar mass function down to the low mass end (Guo et al. 2011, Kang et al. 2012), cold gas mass function (Fu et al. 2013), and some scaling relations like the Tully-Fisher relation (Guo et al. 2011, hereafter G11) and the Faber-Jackson relation (Tonini et al. 2016). However, most (if not all) models cannot reproduce the color distribution of galaxies. The colors of low-mass satellite galaxies are too red (e.g., Weinmann et al. 2006), and the colors of central galaxies are too blue (Kang et al. 2006). These problems also persist in the model of Guo et al. (2013 hereafter G13) which includes more advanced treatments of gas cooling and star formation in satellite galaxies. The color discrepancy indicates that quenching of low mass galaxies is too strong, while the quenching of massive galaxies is not enough. So, the quenching mechanism might be different in low mass and high mass galaxies: the low-mass red galaxies in models are mainly satellites which are often related to environment quenching, like ram-pressure and tidal stripping. However, Luo et al. (2016) pointed out that this process does not have a purely environmental origin. The blue massive galaxies in models are related to insufficient feedback.

The recent version of the L-Galaxies model (Henriques et al. (2015), hereafter H15) has achieved progress in accurately modeling the color distribution in the model. They use the Markov Chain Monte Carlo (MCMC) method to search parameter space to simultaneously fit the stellar mass function at different redshifts and the overall red fraction of galaxies. Although their success comes as no surprise, it indicates that our understanding of galaxy formation is moving in the right direction. For details on how they succeed in reproducing the two observations, we refer readers to their paper. However, it is still not clear if the H15 model can also reproduce the color distributions of both satellite and central galaxies since the quenching mechanism might be different for satellite and central galaxies.

In this paper, we will compare the model predictions of G13 and H15 in terms of the red fraction of satellite and central galaxies, which is the main goal of our paper. On the other hand, it is well known that star formation quenching is closely related to galaxy morphology in that most red/passive galaxies are bulge dominated (e.g., Kauffmann et al. 2004). We also use data to check the morphology mix in the model.

This paper is organized as follows. In Section 2, we briefly summarize the L-Galaxies models and describe the main modifications in H15. In Section 3, we analyze galaxy quenching in H15, comparing them to the G13 model and the SDSS data, such as: quenching fraction, morphology of central galaxies, conditional stellar mass functions and the stellar mass-halo mass (SMHM) relation. In Section 4, we summarize our results and discuss possible improvements.

2 THE L-GALAXIES SEMI-ANALYTIC MODELS

In this section, we briefly introduce the L-Galaxies models and the simulation they use, then describe the main changes in H15 compared to G13.

2.1 The Models and Simulations

L-Galaxies is one of the most successful semi-analytic galaxy formation models. It has been continuously developed by Kauffmann et al. (1999); Springel et al. (2001); Croton et al. (2006); De Lucia & Blaizot (2007) in the last two decades. Recently, the L-Galaxies model of G11 and G13 was improved comprehensively which can reproduce observed galaxy populations well from dwarf spheroidals to cD galaxies. Fu et al. (2010, 2013) developed a model in which the cold gas is partitioned into atomic and molecular components. Yates & Kauffmann (2014) adopted a more realistic model for chemical evolution. After that, H15 published the latest version of L-Galaxies, which is claimed to match the observed evolution of stellar mass function, galaxy colors and star-formation rates, in the *Planck* cosmology. In this work we will use data produced from the G13 and H15 models.

Both the G13 and H15 models are implemented in two N-body simulations: Millennium (hereafter MS, Springel et al. 2005) and Millennium-II (hereafter MS-II, Boylan-Kolchin et al. 2009). Both simulations use cosmological parameters from the first-year WMAP

data and 2160^3 particles. The simulation box of MS is $500\,\mathrm{Mpc\,h^{-1}}$, and MS-II has a box size of $100\,\mathrm{Mpc\,h^{-1}}$, so it has 125 times higher mass resolution than MS. Using the technique developed by Angulo & White (2010) and Angulo & Hilbert (2015), G13 rescaled the cosmological parameters from WMAP1 to WMAP7: $\Omega_\Lambda = 0.728$, $\Omega_m = 0.272$, $\Omega_{\rm baryon} = 0.045$, $\sigma_8 = 0.807$ and $h = 0.704$, while H15 rescaled them to *Planck* cosmology: $\Omega_\Lambda = 0.685$, $\Omega_m = 0.315$, $\Omega_{\rm baryon} = 0.0487$, $\sigma_8 = 0.829$ and $h = 0.673$.

H15 applied the MCMC procedure to find the best parameters by fitting to a series of fiducial observational data: the evolution of stellar mass function and the passive galaxy fraction as a function of stellar mass from $z = 0$ to $z = 3$. Both galaxy catalogs from H15 and G13 are publicly available from the Millennium data base. [1]

2.2 The Main Modifications in the H15 Model

Compared to G13, H15 modified a few treatments of baryonic processes to best fit the observed evolution of star-formation rates, colors and stellar mass up to $z = 3$. For more details about the modifications, please refer to the supplementary material in H15. Here we list the main modifications by H15 compared to the G13 model.

(i) Delay the reincorporation rate of ejected gas into the halo: changing the ejected gas reincorporation rate from $\dot{M}_{\rm ejec} \propto -V_{\rm vir}/t_{\rm dyn,h}$ to $\dot{M}_{\rm ejec} \propto -M_{\rm vir}$. This change leads to a slower gas reincorporation rate in low-mass halos and a quicker reincorporation rate in massive halos.

(ii) Decrease the threshold density for star formation: changing the gas density threshold $\Sigma_{\rm SF}$ from $3.8 \times 10^9 M_\odot\ \mathrm{pc^{-2}}$ to $2.6 \times 10^9 M_\odot\ \mathrm{pc^{-2}}$. In this way a satellite galaxy that is poor in gas can still form stars.

(iii) Ignoring the ram-pressure stripping in less massive halos: setting a ram-pressure threshold $M_{r.p.} = 1.2 \times 10^{14}\ M_\odot$. In this way, the hot gas of satellites in low-mass halos is not stripped and available for continuous cooling and star formation.

(iv) Increasing the radio-mode AGN feedback: the new efficiency of hot gas accretion onto the central black hole, $\kappa_{\rm AGN}$, is equivalent to the one in G13 divided by a factor of $H(z)$. The larger accretion efficiency in H15 leads to quicker growth of a black hole and a stronger AGN feedback (which is related to the gas accretion rate). So, suppression of gas cooling in intermediate and massive galaxies is stronger in the H15 model.

[1] *http://gavo.mpa-garching.mpg.de/Millennium*

3 MODEL PREDICTIONS

In this section, we compare the model predictions of H15 and G13 to the data on the red fraction of central and satellite galaxies, the fraction of galaxies with different morphology, and the stellar mass to halo mass relation.

3.1 Quenched Fraction of Satellites and Central Galaxies

Luo et al. (2016) compared the quenched fraction with SDSS DR7 data, based on the model of Fu et al. (2013). In agreement with previous results they also found that there are too many low-mass quenched satellites and too few quenched central galaxies. Since H15 have fitted the fraction of passive (quenched) galaxies as a function of stellar mass and redshift, now we check this fraction more carefully in this section.

Following Luo et al. (2016), we define galaxies with specific star formation rate $\mathrm{sSFR} < 10^{-11}\ \mathrm{yr^{-1}}$ as quenched galaxies and select galaxies with $\log_{10}\ M_*/M_\odot > 9.5$ from H15. The data points are from Luo et al. (2016) using the MPA-JHU SDSS DR7 catalog and Yang et al. (2007) group catalog with $M_* > 10^{9.5}\,M_\odot$ at $z < 0.04$ and $M_* > 10^{10}\,M_\odot$ at $z = 0.04 \sim 0.06$.

In Figures 1 and 2, we plot the quenched fraction of galaxies at fixed halo mass and fixed stellar mass, but for central galaxies and satellites separately.

By looking at Figures 1 and 2, we find that compared to the G13 model, the H15 model is able to reproduce the red fraction of central galaxies (right panel in Fig. 1) and that of low-mass satellite galaxies with $\log_{10} M_*/M_\odot < 10$ (left panel in Fig. 2). The improvement is slightly better in the MS-II simulation. Compared to the G13 model, H15 increase the quenched fraction of central galaxies significantly at $\log_{10} M_*/M_\odot > 10$, suggesting that increasing the AGN feedback does play more of a role in quenching massive galaxies. However at $\log_{10} M_*/M_\odot < 10$, the quenching fractions of central galaxies from H15 and G13 models are similar, but AGN feedback is not efficient.

Figure 2 is more interesting. It shows that H15 can reproduce the fraction of red satellites at the low-mass end (left panel), but at intermediate stellar mass of $\log_{10} M_*/M_\odot = [10, 11]$ (middle two panels) the red fraction is still lower than what comes from the data. This prediction is very similar to that from the G13 model using MS. In the G13 model, the overprediction of blue satellites at this mass scale can be understood because the central galaxies are also bluer. However, the blue fraction of centrals in the H15 model now agrees with

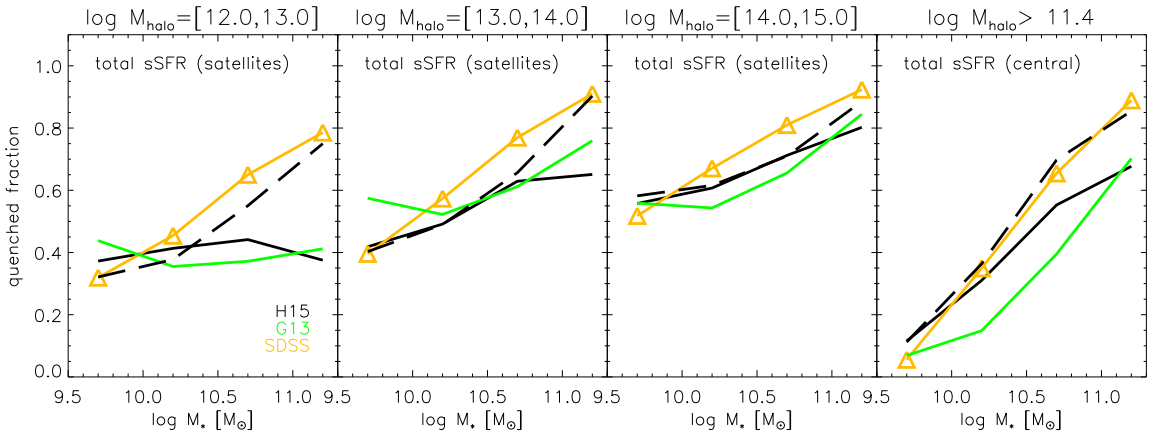

Fig. 1 The quenched fraction of galaxies as a function of stellar mass: the *left three panels* are for satellite galaxies in different halo mass bins, and the *rightmost panel* is for central galaxies in all halos with masses greater than $10^{11.4}M_{\odot}$. These panels show results when quenched galaxies are defined using sSFRs which are corrected to total star formation rates. In each panel, the *triangles* are the SDSS data and the *colored lines* are different model predictions (*solid* for MS and *dashed* for MS-II results).

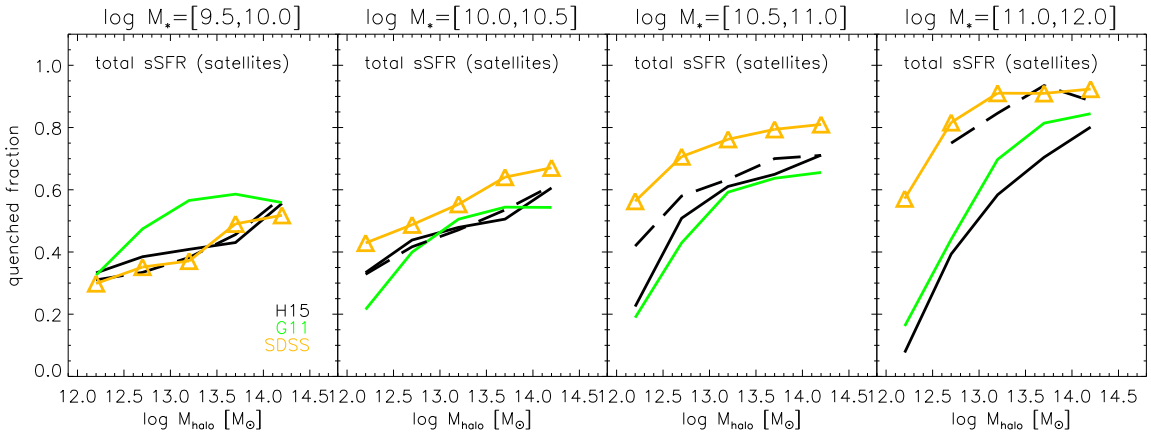

Fig. 2 Same as in Fig. 1, but now quenched fractions are plotted as a function of halo mass in different stellar bins.

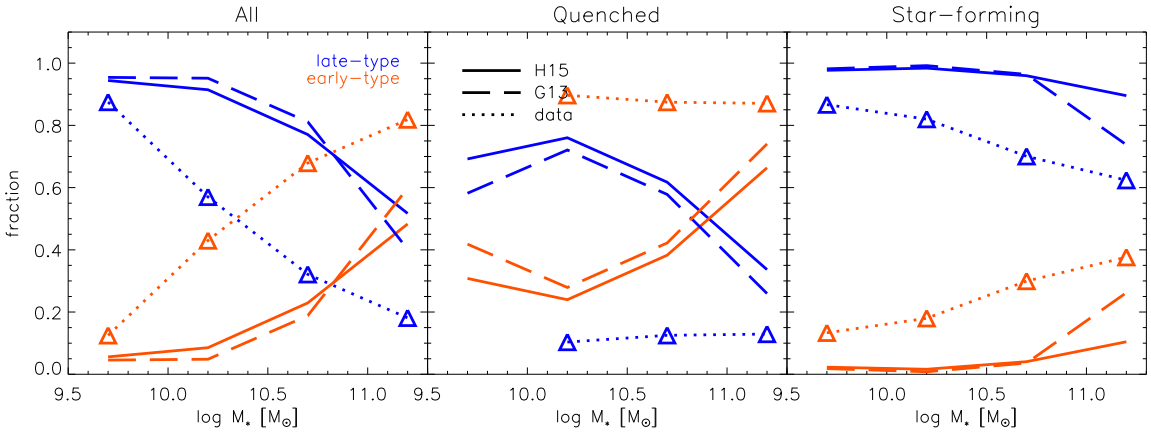

Fig. 3 The fraction of central galaxies' morphology as a function of stellar mass. The *left panel* is for all central galaxies, *middle panel* is for quenched central galaxies, and the *right* panel is for star-forming central galaxies. *Red* corresponds to early-type fractions and *blue* represents late-type fractions. *Triangles* are the SDSS data.

the data. We will later see from Figures 4 and 5 that the stellar mass of centrals at $z = 0$ in the H15 model is actually lower than the data at the given halo mass. This is because they tune the model parameters to fit the stellar mass functions at high redshift and the overall red fraction by introducing strong AGN feedback in massive galaxies and a longer reincorporation time of gas in low mass galaxies. In order to fit the total SMF at $z = 0$, H15 increase the star formation efficiency in satellites by lowering the star formation threshold and ignoring ram pressure stripping in halo mass less than $\log_{10} M_{\rm vir}/M_\odot < 14$. But by doing so, the intermediate stellar-mass galaxies are now bluer.

The correct color of central galaxies and the too blue color of intermediate stellar-mass satellites ($\log_{10} M_*/M_\odot = [10, 11]$) in the H15 model mean that star formation efficiency should be slightly lower for them. This could be achieved by using a threshold as a function of galaxy mass, or including ram-pressure stripping of hot gas in intermediate stellar-mass satellites.

At most massive stellar mass bins (right panel in Fig. 2), there is a significant discrepancy for the quenched fraction of satellites between MS and MS-II (solid and dashed lines respectively). The problem in SAMs might be due to the inconsistent description of physics for satellites whose subhalos cannot be resolved in a simulation, or the different merger history since the merger trees of some massive halos may be not well resolved at higher redshifts in low resolution simulations. This problem has been discussed in detail in Luo et al. (2016).

3.2 The Morphology of Central Galaxies

It is well known that star formation activity is closely related to galaxy morphology (e.g., Kauffmann et al. 2004), so the morphology is also a good indicator of whether a galaxy is passive or star forming. As the H15 model now fits the quenched fraction of central galaxies, it would be interesting to check if they are able to predict the morphology of galaxies. In the following we study the fraction of galaxies divided into ellipticals and spirals.

In the SAMs, every galaxy has a disk plus a bulge, so we use $B/T = M_{\rm Bulge}/M_{\rm total}$ to define the morphology of the galaxy. Normally, galaxies with $B/T \geq 0.7$ are bulge dominated (i.e. elliptical galaxies), those with $0.7 > B/T \geq 0.03$ are normal spirals, and those with $B/T < 0.03$ are pure disks (see sect. 3.8 in G11). Similarly, in SDSS there is a photometric parameter $f_{\rm deV}$ to determine the galaxy morphology. In SDSS, the surface luminosity distribution of each galaxy is a linear combination of exponential and de Vaucouleurs profiles, and $f_{\rm deV}$ is the coefficient of the de Vaucouleurs term. Therefore $f_{\rm deV}$ is most similar to B/T, which reflects the contribution of the bulge component to the whole galaxy. Bernardi et al. (2005) used $f_{\rm deV} > 0.8$ to define early-type (i.e. elliptical) galaxies. Shao et al. (2007) used $f_{\rm deV} < 0.5$ to define spiral galaxies. In this work, we use $B/T \geq 0.7$ as the criterion of early-type galaxies for SAMs, while using $f_{\rm deV} \geq 0.7$ at the r-band as the criterion of early-type galaxies for our SDSS sample (the same sample as Sect. 3.1). Correspondingly, the galaxies with $B/T < 0.7$ or $f_{\rm deV} < 0.7$ are selected as late-type galaxies.

In Figure 3, we plot the fraction of central galaxies' morphology as a function of stellar mass. Red curves are for early-type (elliptical) galaxies and blue curves are for late-type (spirals) galaxies. Solid and dashed curves are the results from H15 and G13 respectively; dotted curves with triangles are the results from our SDSS sample. The left panel is the results for all the galaxies; the middle and right panels are for quenched and star-forming galaxies respectively.

From the left panel, we find H15 and G13 have almost the same morphology fractions and trend for the whole sample: early-type/late-type galaxy fraction increases/decreases with stellar mass. However, that is different from the SDSS data. There are more early-type central galaxies and less late-type central galaxies in the data than H15 and G13 models at $\log_{10} M_*/M_\odot > 10$. Furthermore, in the data early-type is the majority in central galaxies at $\log_{10} M_*/M_\odot > 10.3$, while for the H15 and G13 models late-types are the majority for all stellar masses. This indicates that galaxy morphology in the two models is quite different from the SDSS data: there are more late-type central galaxies in models than in the SDSS.

We further divide the sample into quenched and star-forming galaxies to examine the morphology fraction. For quenched central galaxies (middle panel), the early-type fraction is almost 90% at $\log_{10} M_*/M_\odot > 10$ in SDSS, yet it is totally different in the H15 and G13 models: early-type dominates only at $\log_{10} M_*/M_\odot > 11$. Even the fraction trends are different between SDSS and models: the fraction in SDSS does not change with stellar mass. Comparing H15 with G13, we find their results are quite similar, and there are slightly more late-type and less early-type central galaxies in H15 than what is in G13. This implies there are slightly more late-type galaxies quenched in the H15 model. For star-forming central galaxies, the trends of fractions are quite similar, whereas

in the models there are still more (at least 10%) late-type central galaxies than in SDSS.

We can then conclude that the H15 model has the correct fraction of quenched central galaxies, but the quenching mechanism in H15 may not be correct. It seems that the H15 model quenches too many late-type central galaxies in the stellar mass range of $\log_{10} M_*/M_\odot = [10, 11]$. In the H15 model the quenching is mainly by increasing the efficiency of AGN feedback, not related to the increasing formation of a bulge. We think that a more efficient quenching should be related to the mass growth in the bulge and will discuss this in the last section.

3.3 The Conditional Stellar Mass Functions

The conditional stellar mass function (CSMF, firstly proposed by Yang et al. 2003) describes the average number of galaxies as a function of stellar mass in dark matter halos of given mass. The CSMF, which is closely related to correlation functions, provides additional constraints on galaxy formation and evolution, as in principle the formation of dark matter halos depends on their mass, so their galaxy population should be different. Kang et al. (2012) have shown that CSMFs in the G13 model are inconsistent with the data by producing more stellar mass in satellite galaxies. Since the H15 model provides better fits to the observed SMFs at different redshifts and the correct fraction of quenched central galaxies, it is worthwhile to check their model predictions on the CSMFs.

In Figure 4, we show the CSMFs in different halo mass bins, and separate the contributions from central (blue curves) and satellite (red curves) galaxies. The solid and dashed lines are for H15 and G13 models respectively, and the data points are from Yang et al. (2012) which is measured from their constructed group catalog using SDSS DR7.

We find that the CSMFs of satellite galaxies in the H15 model are in good agreement with the SDSS data throughout the whole halo mass, and they are lower than the results of G13 by at least 0.2 dex at low stellar mass ends. But for central galaxies, except for the highest halo mass bins $\log_{10} M_{\rm halo}/M_\odot = [14.25, 14.55]$, the G13 model is more consistent with the SDSS data than the H15 model. The stellar mass of centrals in the H15 model is systematically lower than the data by 0.2–0.3 dex. This is related to the high AGN feedback in the H15 model, which is enhanced by 1 dex compared to the G13 model at $z = 0$, see figure S4 in the supplementary material of H15. This fast quenching leads to a lower stellar mass in the H15 model.

However, the fact that the quenched fraction of central galaxies in H15 is consistent with SDSS data suggests that increasing quenching of central galaxies in the model is necessary. This indicates that we need to quench more central galaxies to match the observed red fraction, but only after the central galaxy has the right amount of stellar mass. It is still not clear how to achieve these two goals at the same time; we will touch on this in the discussion part.

3.4 The Stellar Mass-Halo Mass Relation

In the previous section we found at given halo mass the central galaxies in the H15 model have lower stellar mass than the data. In this section we further compare the prediction of models H15 and G13 to the data by showing their SMHM relation. The SMHM relation is a very basic and important relation for constraining galaxy formation physics. As shown by many others (e.g., Guo et al. 2010; Kang et al. 2012), once this relation is well determined, it would be easy to fit the stellar mass function and galaxy clustering.

We plot the SMHM relations for central galaxies at different redshifts in Figure 5; black lines are from H15, red lines are from G13, and blue lines are from the abundance matching results (Moster et al. 2013). It is found that at $z = 0$ (left panel), at fixed halo mass, stellar mass of H15 is lower than the abundance matching results and G13. At high redshifts (middle and right panels) for massive halos, the stellar mass from H15 and G13 models is similar, except that at $z = 2$ the H15 model predicts a higher stellar mass. For low-mass halos, the stellar mass from H15 is also lower than the G13 model. This is consistent with what H15 did in their model. H15 used the MCMC method to find the best parameters to fit the SMFs at high-z where they predicted slightly more massive galaxies at $z = 2$ (see their fig. 2) so their stellar mass in massive halos at $z = 2$ is higher. But for low-mass halos, they adopted a longer gas reincorporation time to best fit the faint end of SMFs, so their stellar mass is lower than the G13 model.

In the model of H15, the AGN feedback at $z = 0$ is stronger than that of G13, so they are able to produce more red central galaxies, as stated before, to fit the red fraction in the data. This is why their stellar mass in massive halos is lower than both the G13 model and the abundance matching of Moster et al. (2013).

The SMHM relation of Moster et al. (2013) is obtained from abundance matching. It is not the observed halo mass, so in Figure 6 we plot the SMHM relation using the observed data by Mandelbaum et al. (2006) where

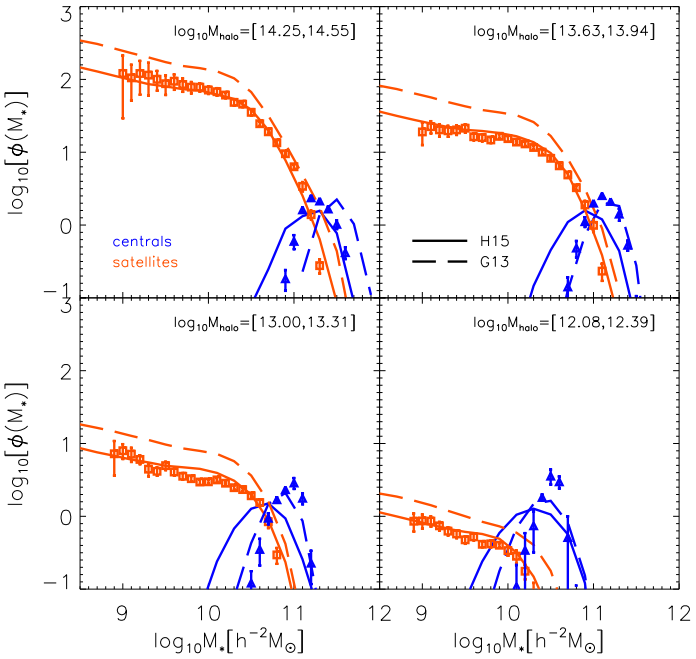

Fig. 4 CSMFs in different halo mass bins. The *solid* curves are from H15 and the *dashed* curves are from G13. The data points are from Yang et al. (2012). The *red/blue* lines are for satellites/central galaxies.

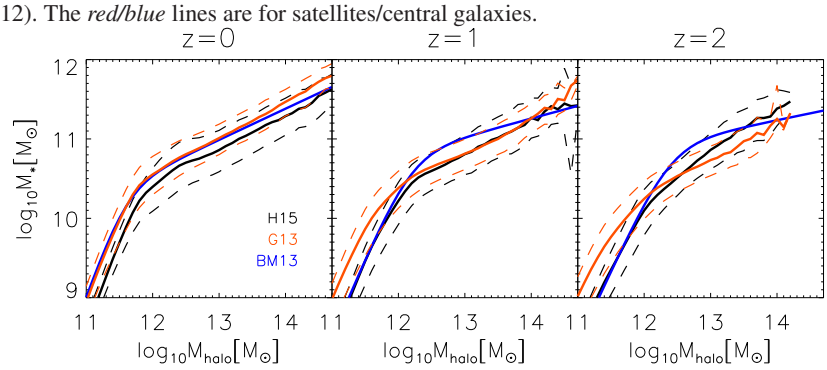

Fig. 5 The SMHM relation at $z = 0, 1, 2$ for central galaxies. The *black* lines are the median value from H15, the *red* lines are the median value from G13, and the *dashed* lines represent the 68 percentile scatter of the models. The *blue* lines are from Moster et al. (2013).

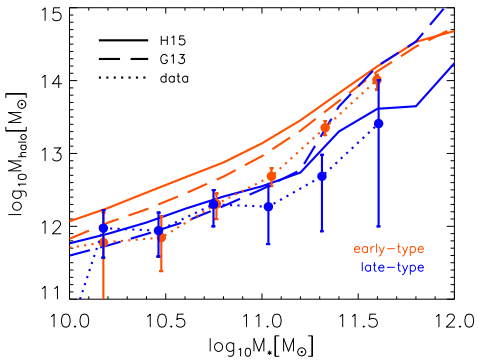

Fig. 6 The SMHM relation at $z = 0$ for central galaxies, but separately for early-type (*red*) and late-type (*blue*) galaxies. The data points with error bars are from Mandelbaum et al. (2006).

the halo mass is measured from the weak lensing results provided by SDSS, which are more reliable. We separated the central galaxy sample into early-type and late-type, and show the results at $z = 0$. Here, early-type is defined as $B/T \geq 0.7$ for the models.

It is easy to see from Figure 6 that at given stellar mass, the early-type galaxies from both G13 and H15 models are higher than the data. We note that there might be some systematic difference in the stellar mass obtained in the models and observations, so we do not focus on the absolute halo mass or stellar mass from this relation. What is more interesting is difference in the SMHM relations for the early-type and late-type galaxies.

Figure 6 shows that in the data (points with error bars) the halo mass of early-type and late-type galaxies is very similar for $\log_{10} M_*/M_\odot < 11$. For more massive galaxies, at given stellar mass the early-type galaxies have higher halo mass. Note that the error bars of late-type galaxies are very large at the high mass end due to their lower number density. However, it is seen that in both the G13 and H15 models, the halo mass of early-type galaxies is higher than in late-type galaxies at given stellar mass, inconsistent with the data at $\log_{10} M_*/M_\odot < 11$. The discrepancy is slightly larger in the H15 model. This indicates that AGN feedback is either overestimated in bulge dominated galaxies or underestimated in disk dominated galaxies. As both the G13 and H15 models have too many disk dominated galaxies, lowering their AGN feedback will lead to more stellar mass growth and will ruin the agreement with the observed SMFs. We thus conclude that it is more likely the AGN feedback in both models is too strong, and is comparatively stronger in the H15 model.

4 CONCLUSIONS AND DISCUSSION

In this paper, we compare predictions from the two latest versions of the L-Galaxies model, H15 and G13, to SDSS data. The H15 model has introduced a few modifications to the G13 model and is tuned to better match the evolution of the stellar mass function and the fraction of red galaxies as a function of stellar mass. By comparing the model predictions to data in more detail, we have obtained the following results.

(I) We examine the quenched fraction of central galaxies and satellites separately. It is found that, compared to the overprediction of blue central galaxies in G13, the H15 model can reproduce the red fraction of central galaxies. The overprediction of low-mass red satellites is also solved in the H15 model to match the data. However, the quenched fraction of satellite galaxies at $\log_{10} M_*/M_\odot = [10, 11]$ in both G13 and H15 models is still lower than the SDSS data.

(II) We check the morphology of central galaxies. We find there are too many late-type galaxies and too few early-type galaxies in both G13 and H15 models compared to the SDSS data. In addition, too many late-type galaxies in H15 at $\log_{10} M_*/M_\odot = [10.0, 11.0]$ are quenched.

(III) We examine the stellar mass function of central and satellite galaxies in different halo mass bins, and find that H15 produce a better match to the observed stellar mass function of satellites than the G13 model, but the match to the stellar mass of centrals is worse than G13. The stellar mass of central galaxies is lower by about 0.2 dex than the data suggest.

(IV) We compare the SMHM relation to the data, and find that G13 fit the observed stellar mass-halo mass relation better, and at a given halo mass, the stellar mass of central galaxies in H15 is lower than the data, especially for early-type galaxies.

H15 have clearly shown that a long reincorporation time of SN ejected gas is helpful to suppress the star formation rate in low-mass galaxies, thus providing a better match to the stellar mass function at high redshifts. To solve the excess redness of these low-mass satellite galaxies ($\log_{10} M_*/M_\odot < 10$) they use a lower threshold gas density for star formation and ignore the ram-pressure stripping in low-mass halos. However, we found that such an extension of star formation in satellites produces slightly more blue satellites at $10 < \log_{10} M_*/M_\odot < 11$. This could be solved by using a density threshold as a function of galaxy stellar mass, not a constant like in the current H15 model.

By introducing an AGN feedback parameter which is higher than the G13 one at low redshift, the H15 model can reproduce the red fraction of central galaxies. However, the stellar mass of those quenched central galaxies is now slightly lower (by about 0.2 dex) than the data. Our results also show that in the G13 and H15 models there are too many disk dominated galaxies, and especially too many red disk galaxies. To solve these two problems simultaneously, we need some mechanisms to increase the growth of the bulge component in central galaxies, and the feedback (regardless if from an AGN or another source) from the bulge formation is used to quench the galaxy. In this way, the stellar mass of centrals can be increased to match the data, and we can have more bulge dominated quenched galaxies.

In L-Galaxies, bulge formation occurs through three channels: major mergers, minor mergers and disk in-

stability. For major mergers, two galaxies merge with mass ratio ($m_{\rm sat}/m_{\rm cen}$) larger than 0.3, then all the stars in both galaxies and the newly formed stars during the merger are assumed to form a new bulge. For minor mergers, only the stars in satellites are added into the bulge of the central galaxy. Normally, during a major merger, a strong starburst will consume almost all the cold gas and suppress further star formation. In L-Galaxies, major mergers are better modeled due to their rapid dynamical friction time, so we do not think there is no more space to increase the major merger rate. On the contrary, there is some freedom to increase the minor merger rate, as shown by van Daalen et al. (2016) in which a shorter merger time is really needed to match the galaxy clustering using the H15 model.

Disk instability is another important channel to form a bulge. Due to this dynamic instability, the unstable disk will transfer some stellar mass into a bulge to make the disk stable again. Also, some new stars can form during the instability. G11 have pointed out that disk instability is a major way to form a bulge in intermediate mass galaxies like the Milky Way. This is also the mass range where the bulge grows insufficiently in H15, so increasing the disk instability might be a possible solution. Recently, Tonini et al. (2016) presented a comprehensive theoretical prescription for the growth of disks and bulges in a SAM. They divided the bulges into two populations: merger-driven bulges and instability-driven bulges. Their model can reproduce some observations, such as the mass-size relation and the Faber-Jackson relation. They found that the merger-driven ellipticals are dominant in both low-mass and high-mass ends of stellar mass, while instability-driven bulges dominate the intermediate mass range. These also indicate that increasing the disk instability is a suitable solution to improve the quenching and morphology of central galaxies in SAMs. We expect future solutions will reconcile conflicts between stellar mass functions, color and morphology distributions in SAMs.

Acknowledgements We thank Qi Guo for helpful discussions and Lei Wang for providing the SDSS DR7 catalog. The Millennium Simulation data bases used in this paper and the web application providing online access to them were constructed as part of activities associated with the German Astrophysical Virtual Observatory (GAVO). This work is supported by the National Basic Research Program of China (2015CB857003 and 2013CB834900), the Natural Science Foundation of Jiangsu Province (No. BK 20140050), the National Natural Science Foundation of China (NSFC, No. 11333008) and the Strategic Priority Research Program 'The Emergence of Cosmological Structure' of CAS (No. XDB09010403).

References

Angulo, R. E., & Hilbert, S. 2015, MNRAS, 448, 364
Angulo, R. E., & White, S. D. M. 2010, MNRAS, 405, 143
Bernardi, M., Sheth, R. K., Nichol, R. C., Schneider, D. P., & Brinkmann, J. 2005, AJ, 129, 61
Bower, R. G., Benson, A. J., Malbon, R., et al. 2006, MNRAS, 370, 645
Boylan-Kolchin, M., Springel, V., White, S. D. M., Jenkins, A., & Lemson, G. 2009, MNRAS, 398, 1150
Croton, D. J., Springel, V., White, S. D. M., et al. 2006, MNRAS, 365, 11
De Lucia, G., & Blaizot, J. 2007, MNRAS, 375, 2
Frenk, C. S., & White, S. D. M. 2012, Annalen der Physik, 524, 507
Fu, J., Guo, Q., Kauffmann, G., & Krumholz, M. R. 2010, MNRAS, 409, 515
Fu, J., Kauffmann, G., Huang, M.-l., et al. 2013, MNRAS, 434, 1531
Guo, Q., White, S., Li, C., & Boylan-Kolchin, M. 2010, MNRAS, 404, 1111
Guo, Q., White, S., Boylan-Kolchin, M., et al. 2011, MNRAS, 413, 101
Guo, Q., White, S., Angulo, R. E., et al. 2013, MNRAS, 428, 1351
Henriques, B. M. B., White, S. D. M., Thomas, P. A., et al. 2015, MNRAS, 451, 2663
Kang, X., Jing, Y. P., Mo, H. J., & Börner, G. 2005, ApJ, 631, 21
Kang, X., Jing, Y. P., & Silk, J. 2006, ApJ, 648, 820
Kang, X., Li, M., Lin, W. P., & Elahi, P. J. 2012, MNRAS, 422, 804
Kauffmann, G., Colberg, J. M., Diaferio, A., & White, S. D. M. 1999, MNRAS, 303, 188
Kauffmann, G., White, S. D. M., Heckman, T. M., et al. 2004, MNRAS, 353, 713
Luo, Y., Kang, X., Kauffmann, G., & Fu, J. 2016, MNRAS, 458, 366
Mandelbaum, R., Seljak, U., Kauffmann, G., Hirata, C. M., & Brinkmann, J. 2006, MNRAS, 368, 715
Moster, B. P., Naab, T., & White, S. D. M. 2013, MNRAS, 428, 3121
Schaye, J., Crain, R. A., Bower, R. G., et al. 2015, MNRAS, 446, 521
Shao, Z., Xiao, Q., Shen, S., et al. 2007, ApJ, 659, 1159
Somerville, R. S., Hopkins, P. F., Cox, T. J., Robertson, B. E., & Hernquist, L. 2008, MNRAS, 391, 481
Somerville, R. S., & Primack, J. R. 1999, MNRAS, 310, 1087

Springel, V., White, S. D. M., Tormen, G., & Kauffmann, G. 2001, MNRAS, 328, 726
Springel, V., White, S. D. M., Jenkins, A., et al. 2005, Nature, 435, 629
Tonini, C., Mutch, S. J., Croton, D. J., & Wyithe, J. S. B. 2016, MNRAS, 459, 4109
van Daalen, M. P., Henriques, B. M. B., Angulo, R. E., & White, S. D. M. 2016, MNRAS, 458, 934
Vogelsberger, M., Genel, S., Springel, V., et al. 2014, MNRAS, 444, 1518
Weinmann, S. M., van den Bosch, F. C., Yang, X., et al. 2006, MNRAS, 372, 1161
White, S. D. M., & Frenk, C. S. 1991, ApJ, 379, 52
Yang, X., Mo, H. J., & van den Bosch, F. C. 2003, MNRAS, 339, 1057
Yang, X., Mo, H. J., & van den Bosch, F. C. 2007, MNRAS, 671, 153
Yang, X., Mo, H. J., van den Bosch, F. C., Zhang, Y., & Han, J. 2012, ApJ, 752, 41
Yates, R. M., & Kauffmann, G. 2014, MNRAS, 439, 3817